ground water

Implications of Rate-Limited Mass Transfer for Aquifer Storage and Recovery

by Sean L. Culkin[1], Kamini Singha[2], and Frederick D. Day-Lewis[3]

Abstract

Pressure to decrease reliance on surface water storage has led to increased interest in aquifer storage and recovery (ASR) systems. Recovery efficiency, which is the ratio of the volume of recovered water that meets a predefined standard to total volume of injected fluid, is a common criterion of ASR viability. Recovery efficiency can be degraded by a number of physical and geochemical processes, including rate-limited mass transfer (RLMT), which describes the exchange of solutes between mobile and immobile pore fluids. RLMT may control transport behavior that cannot be explained by advection and dispersion. We present data from a pilot-scale ASR study in Charleston, South Carolina, and develop a three-dimensional finite-difference model to evaluate the impact of RLMT processes on ASR efficiency. The modeling shows that RLMT can explain a rebound in salinity during fresh water storage in a brackish aquifer. Multicycle model results show low efficiencies over one to three ASR cycles due to RLMT degrading water quality during storage; efficiencies can evolve and improve markedly, however, over multiple cycles, even exceeding efficiencies generated by advection-dispersion only models. For an idealized ASR model where RLMT is active, our simulations show a discrete range of diffusive length scales over which the viability of ASR schemes in brackish aquifers would be hindered.

Introduction

As the world's population continues to grow, so does the importance of water as a natural resource. Per capita water use is increasing, especially in areas with low or marginal access to ground water (Gleick 2000). New water management strategies are needed to meet this increasing demand in an efficient and sustainable way. Aquifer storage and recovery (ASR), where excess surface or municipal water is injected into subsurface aquifers for later recovery, is one promising strategy for managing surplus water and overcoming water shortages (Pyne 1995). The recharged water may be stored for use during an emergency, to offset periods of water deficit, or to augment efforts to limit salt water intrusion in coastal areas (Brothers and Katzer 1990; Pyne 1995; Campbell et al. 1997; Petkewich et al. 2004). The ASR injection displaces the native aquifer fluid, creating a reservoir of potable or nearly potable water that can be used later (Eastwood and Stanfield 2001).

ASR is a promising technology because it (1) reduces the need for standard treatment and production facilities; (2) minimizes the need for additional infrastructure such as aboveground storage tanks or reservoirs; (3) requires only minimal treatment of recovered water; and (4) is assumed not to degrade the native ground water quality (Mirecki et al. 1998). The reason underlying the increasing interest in ASR is that it constitutes a sustainable, and often inexpensive, way to develop ground water resources, especially in ground water poor areas. Water can be stored during periods of low demand and recovered when demand is high, such as during peak summer water usage in a hot climate (Brothers and Katzer 1990).

The success of an ASR scheme is normally measured in terms of recovery efficiency, which is defined as the percentage of water injected into a system in an ASR site

[1]Corresponding author: Department of Geosciences, Pennsylvania State University, Deike Building, University Park, PA 16802; (510) 628-3223; fax: (510) 451-3165; sean.culkin@gmail.com

[2]Department of Geosciences, Pennsylvania State University, Deike Building, University Park, PA 16802; ksingha@geosc.psu.edu

[3]U.S. Geological Survey, Office of Ground Water, Branch of Geophysics, 11 Sherman Pl., Unit 5015, Storrs, CT 06269; daylewis@usgs.gov

Received July 2007, accepted January 2008.

doi: 10.1111/j.1745-6584.2008.00435.x

that fulfills the targeted water quality criteria when recovered. In most hydrogeologic settings, the simplistic "underground storage tank" conceptual model applied to ASR systems may have limited utility. Multiple processes—physical, chemical, and biologic, all of which can degrade water quality—control ASR efficiency. A numerical modeling study of three ASR sites in Wisconsin found that dispersive mixing was the most important factor controlling efficiency (Lowry 2004; Lowry and Anderson 2006); heterogeneity and preferential flow, however, may result in nondispersive mixing processes. For example, solute can be transported between mobile and less mobile domains by rate-limited mass transfer (RLMT) (e.g., Pedit and Miller 1994; Haggerty and Gorelick 1995), which could impact efficiency. The rate of mass transfer between domains is determined by flow velocity, permeability, diffusive length scale, and molecular diffusion. RLMT has been shown to occur in multiple settings, including (1) fractured bedrock, where advective transport dominates in fracture conduits and diffusive exchange occurs between the surrounding matrix rock and the fractures (e.g., Fleming and Haggerty 2001; Haggerty et al. 2001; Zheng and Bennet 2002); (2) heterogeneous glacial and fluvial deposits (e.g., Harvey et al. 1994; Feehley et al. 2000; Zheng and Bennet 2002); and (3) soil where preferential flow occurs in macropores (e.g., van Genuchten and Wierenga 1976; Rao et al. 1980; Haggerty and Gorelick 1998; Haws et al. 2004).

In the context of aquifer remediation, RLMT imposes severe limitations on the efficiency of pump-and-treat schemes because immobile contamination diffuses slowly into the mobile domain from which pumping occurs. Such limitations can result in longer-than-anticipated cleanup times (e.g., Haggerty and Gorelick 1995). Similarly, in the context of ASR, RLMT has the potential to degrade efficiencies if immobile saline or brackish fluids are in hydraulic connection with mobile injected fresh water during injection and storage. The effect of nondispersive mixing processes such as RLMT on ASR systems has received little attention; furthermore, few studies (e.g., Barker et al. 2000) have used models in conjunction with field data to explore the evolution of efficiency at specific ASR sites. Given the emergence of ASR as an important strategy in water resource development, quantifying the effects of processes such as RLMT on ASR efficiency and efficacy is needed.

In this study, we use numerical flow and transport modeling in combination with field-scale experimental data from Charleston, South Carolina, to test the hypothesis that ASR efficiency is affected by RLMT. We focus on efficiency as our main criterion for testing the viability of ASR. Although our efforts primarily are focused on modeling the Charleston site, our results are general and point to the need to quantify mass transfer processes for evaluation and design of ASR operations.

ASR Efficiency

Primary or secondary drinking water standards for one or more dissolved solutes in the recovered water are often used to define efficiency (e.g., Petkewich et al. 2004). Salinity is a common limiting constituent, but various metals or compounds may be more appropriate depending on site-specific conditions. The ideal ASR system would substitute subsurface storage for an aboveground water tank and recover 100% of the injectant as potable water. It is unlikely, however, that such a scenario is possible in aquifer systems (1) containing nonpotable pore fluids; (2) where regional ground water flow may cause migration of the fresh water bubble; or (3) where injected water is subject to degradation in quality by biogeochemical changes (e.g., Ma and Spalding 1996; Mirecki et al. 1998; Parkhurst and Petkewich 2001; Gaus et al. 2002; Petkewich et al. 2004; Vanderzalm et al. 2002; Herczeg et al. 2004; Le Gal La Salle et al. 2005). Although biological processes may be limited to the immediate vicinity of the wellbore, changes in water quality due to interaction with the rock matrix and native water can occur at great distances from the injection (Le Gal La Salle et al. 2005). Mixing with native pore fluids is the primary mechanism by which injected water is degraded at the Charleston site (Petkewich et al. 2004). In cases where only advection and dispersion processes are considered, mixing is confined to the edge of the injected fresh water bubble. With considerations of RLMT, nondispersive mixing may occur within the fresh water bubble as chemicals exchange locally between overlapping mobile and immobile domains.

Rate-Limited Mass Transfer

RLMT has been used to explain solute transport in the subsurface where traditional advection-dispersion models are inadequate. Laboratory-scale experiments on heterogeneous samples have shown non-Fickian behavior such as early breakthrough and long tailing of tracers in a variety of hydrogeologic settings (e.g., Haselow and Greenkorn 1991; Haws et al. 2004). Even in relatively homogeneous aquifer material such as well-sorted sand, studies have found evidence for preferential flow paths and multiple rates of mass transfer (Haggerty and Gorelick 1995). Migrating contaminant plumes may linger for prolonged periods because of stagnation in immobile pore spaces. Similarly, rebounding of concentration following injection or pumping may be linked with RLMT (e.g., Harvey et al. 1994; Haggerty et al. 2001; Singha et al. 2007). RLMT is of primary importance to this study, because exchange of solute within the bubble of injected water may impact efficiencies at ASR sites.

Dual-domain porosity models (DDM), also known as bicontinuum models, have been used to simulate RLMT in a number of settings, including agricultural field soils and unconfined, alluvial aquifers (e.g., Coats and Smith 1964; van Genuchten and Wierenga 1976; Griffioen et al. 1998; Feehley et al. 2000; Haggerty et al. 2001; Molz et al. 2006). The DDM differs from the commonly used single-domain porosity advection-dispersion model (SDM) in that a representative elementary volume comprises two interacting zones: (1) a mobile domain where advection and dispersion occur and (2) an immobile domain where advective transport does not occur (e.g., Haggerty and Gorelick 1995; Griffioen et al. 1998; Flach et al. 2004). This system is expressed by (modified from van Genuchten and Wierenga 1976):

$$\theta_m \frac{\partial C_m}{\partial t} + \theta_{im} \frac{\partial C_{im}}{\partial t} = \nabla \cdot (\theta_m \mathbf{D} \cdot \nabla C_m) - \nabla \cdot (\mathbf{q} C_m) + q_s C_s \quad (1)$$

$$\theta_{im} \frac{\partial C_{im}}{\partial t} = \beta (C_m - C_{im}) \quad (2)$$

where C_m = the concentration of mobile pore fluids [M/L^3], C_{im} = the concentration of immobile pore fluids [M/L^3], C_s = the concentration of sink/source fluids [M/L^3], t = time [T], θ_m = the mobile porosity [—], θ_{im} = the immobile porosity [—], $\mathbf{D}$ = the dispersion coefficient [L^2/T], $\mathbf{q}$ = the vector of Darcy velocities [L/T], q_s = the volumetric flow rate from sink/sources [/T], and β = the mass exchange rate coefficient between the mobile and the immobile porosity domain [/T].

Equation 2 describes the first-order rate law by which solute transfer occurs between the mobile and the immobile porosity domains (van Genuchten and Wierenga 1976) where the total porosity $\theta_t = \theta_m + \theta_{im}$. These parameters should not be confused with total effective porosity (θ_e) in an SDM. The solute exchange rate coefficient, β, is dependent on the length scale of contact between the mobile and the immobile pore fluids. Mass transfer may also depend on fluid velocities and sorption (Griffioen et al. 1998). β can exist as a single transfer coefficient that links two discrete porosity zones in a DDM or as a statistical distribution of diffusive pore length scales (Haggerty et al. 2001). The model acts as a single-porosity domain when β becomes either high or low relative to the scale of the system. For low β values, virtually no solute is exchanged between the two domains, so the immobile zone is nullified and the system acts similar to a SDM where $\theta_e \approx \theta_m$. For high β values, solute exchange becomes virtually instantaneous, such that the two porosity zones are evenly mixed and act as a single domain where $\theta_e \approx \theta_t$.

Site Description and Previous Work

Two pilot-scale ASR projects were conducted in Charleston, South Carolina: one between 1993 and 1995 (Campbell et al. 1997) and other between 1998 and 2002. Charleston relies primarily on surface water sources for drinking water (Petkewich et al. 2004), and concern over damage or contamination to the surface water supply as a result of flooding, hurricanes, and other natural disasters led to the installation of an ASR system (Figure 1) by the Charleston Commissioners of Public Works and evaluation by the USGS (Mirecki et al. 1998; Petkewich et al. 2004).

The 1993 to 1995 ASR tests were conducted at the "pilot study" site, west of the main Charleston peninsula, and the 1998 to 2002 "phase II" tests were done about 3 km to the east, on the main Charleston peninsula (Figure 1). The geology at both ASR sites is similar except for minor differences in formation depths: the sites consist of approximately 760 m of Upper Cretaceous through Quaternary age sedimentary rocks that are underlain by Precambrian and Paleozoic basalt (Petkewich et al. 2004). The fractured-rock aquifer targeted for ASR evaluation is the Black Mingo Group, a Tertiary-age marginal marine and inner shelf deposit. The Black Mingo group is overlain by the Eocene Santee Limestone, a quartz-rich fossiliferous limestone. These two formations act as a single hydrogeologic unit between depths of about 116 and 137 m below the land surface and are referred to as the Black Mingo/Santee Limestone (BM/SL) Aquifer (Campbell et al. 1997). Figure 2 shows a generalized schematic of the hydrogeology at the pilot study site. Electromagnetic flowmeter data indicate two main productive zones in the BM/SL Aquifer, an upper zone located at 116 to 122 m below the land surface and a lower zone at 131 to 137 m (Figure 2); these highly fractured zones account for 49% and 40% of total flow in the aquifer, respectively (Campbell et al. 1997; Mirecki et al. 1998; Petkewich et al. 2004). Underlying the BM/SL Aquifer are consolidated silty muds, which form a lower confining unit at about 137 m depth (Campbell et al. 1997). Above the BM/SL Aquifer is the upper unconfined aquifer, which extends down to 20 m below the land surface; these units are laterally continuous for several miles in Charleston. The confined BM/SL Aquifer is saturated with brackish water and predevelopment flow was directed toward the coastline (Aucott and Speiran 1985).

The pilot study site ASR tests consisted of 13 injection, storage, and recovery cycles with varying injection rates, and storage periods between 0 and 144 h. Recovery efficiencies ranged between 38% and 81% (Campbell et al. 1997). The phase II study performed four cycles of injection, storage, and recovery of the ASR system between 1999 and 2002; each cycle consisted of injection of approximately 7 million liters of water for a storage period of 1 to 6 months (Petkewich et al. 2004). For the phase II study, recovery efficiency was between 21% and 34% and did not vary greatly between the shorter and the longer storage test periods. Recovery efficiency was defined by the U.S. EPA secondary standard for chloride (250 mg/L) for both the pilot study site and the phase II site ASR tests. Sodium and sulfate concentrations of the recovered water demonstrate mixing of fresh water and native water. Some salinity rebound was observed in the BM/SL Aquifer during storage in these experiments and was attributed to upconing of salts from adjacent confining units (Petkewich et al. 2004).

Field Experiment

In the summer 2005, we conducted an 11-d cycle of injection, storage, and recovery at the pilot study site used for the 1993 to 1995 tests near the main Charleston peninsula (see pilot study site in Figure 1), approximately 3 km west of the phase II site. Three observation wells, numbered 733, 843, and 844, are arranged around the central ASR injection/pumping well 736. The observation wells are placed at similar radial distances from well 736 and are open through the BM/SL Aquifer and the confining units. Municipal fresh water was injected into the BM/SL Aquifer at a rate of 174 m^3/d for 5 d, stored for 2 d, and recovered at 468 m^3/d for 4 d. Water level, bulk electrical conductivity, and mobile fluid electrical conductivity

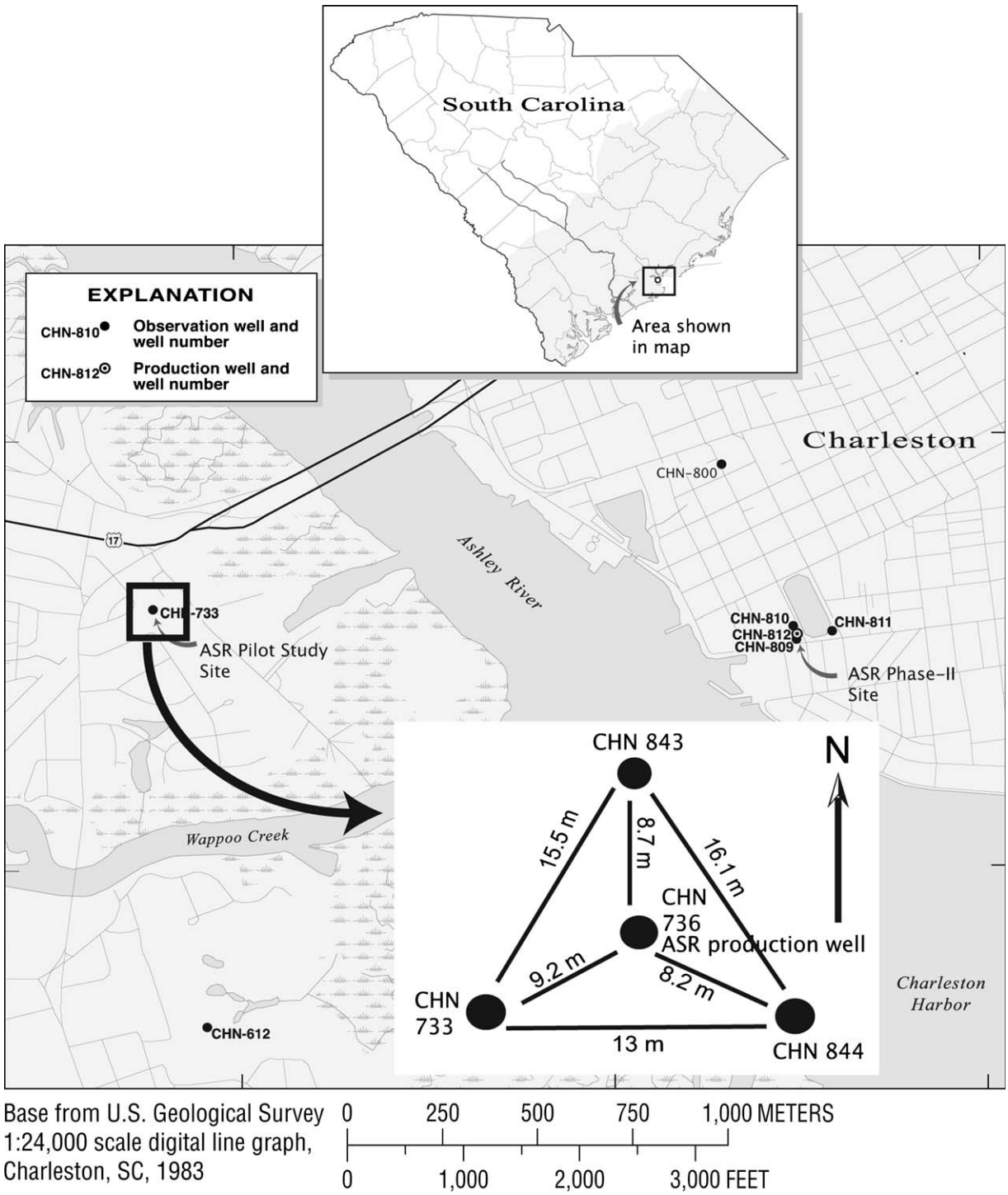

Figure 1. Site map and well configuration for ASR experiment, Charleston, South Carolina. A total volume of 870 m^3 of water was injected at 174 m^3/d over 5 d, stored for 2 d, and recovered at 468 m^3/d over 4 d. Observation wells CHN-733, CHN-843, and CHN-844 are arranged around a central ASR well CHN-736, through which water is injected and recovered. Wellbores are open to the formations below 10 m from ground surface.

were collected from three observation wells over the course of the 11-d ASR cycle.

Fluid samples were taken by low-flow pumping from the two targeted production zones in the three observation wells. A multiparameter probe was used to determine the fluid-specific conductivity, which is used as a proxy for total dissolved solids concentration (TDS) of mobile pore fluids in this study. In the following discussion, we describe data interchangeably as salinity or TDS of fluids in the BM/SL Aquifer. We injected fluid with a salinity of 160 mg/L into the aquifer saturated with a pore fluid salinity of 3300 mg/L.

Drawdown and Salinity Data

Drawdown data show the three phases of the ASR cycle in observation wells 843 and 844 (Figure 3A). Drawdown data are not available from well 733 in this study because of a well liner that precluded head

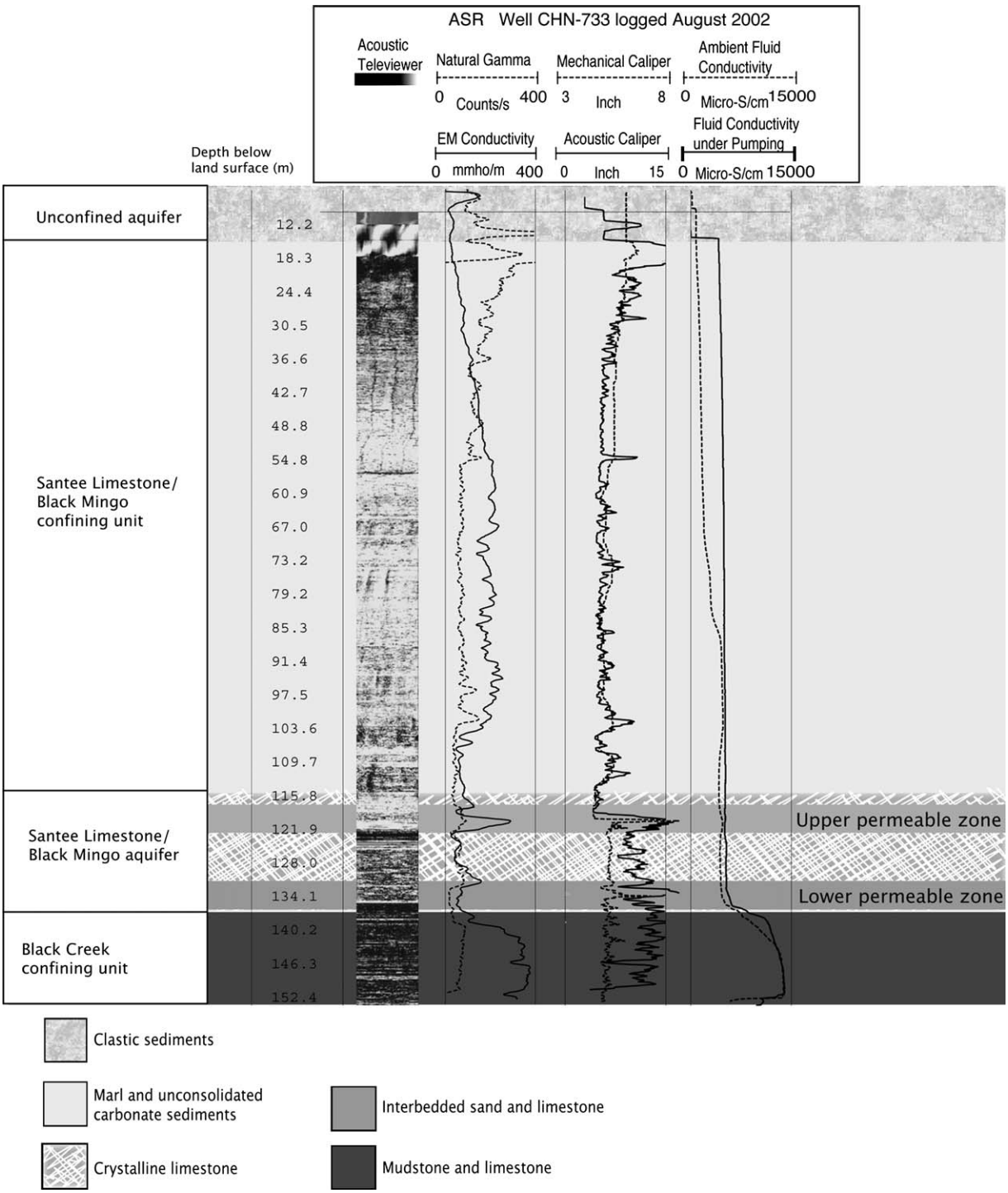

Figure 2. Stratigraphy and geophysical logs for the BM/SL group at the ASR site, Charleston, South Carolina. The BM/SL group is a clastic-limestone unit that acts as a single, confined aquifer. Acoustic televiewer, gamma ray, electromagnetic (EM) (bulk) conductivity, mechanical caliper, acoustic caliper, and fluid conductivity under ambient and pumping conditions were logged from well CHN-733 at the "pilot study" site (Figure 1). Two primary productive zones were located in the BM/SL, at around 116 and 130 m below the ground surface.

measurements. Immediately after the start of injection, both wells recorded a positive gain in hydraulic head above the initial head; when injection ceased, head in both wells recovered quickly (days 6 and 7). The drawdown response from the start of pumping (day 7) until the end of the cycle is an inverted profile of the injection phase data; however, a higher net change in head is achieved during recovery (+6 to 8 m compared to −2 m because of injection) because of a recovery pumping rate that was nearly three times the rate of injection. Although wells 843 and 844 are at a similar radial distance from extraction well 736, less head change is observed at well 843 relative to well 844 during both injection and recovery, suggesting less connectivity between wells 843 and 736.

The three phases of the ASR cycle also are evident in the salinity data (Figure 3B). For an ASR system in

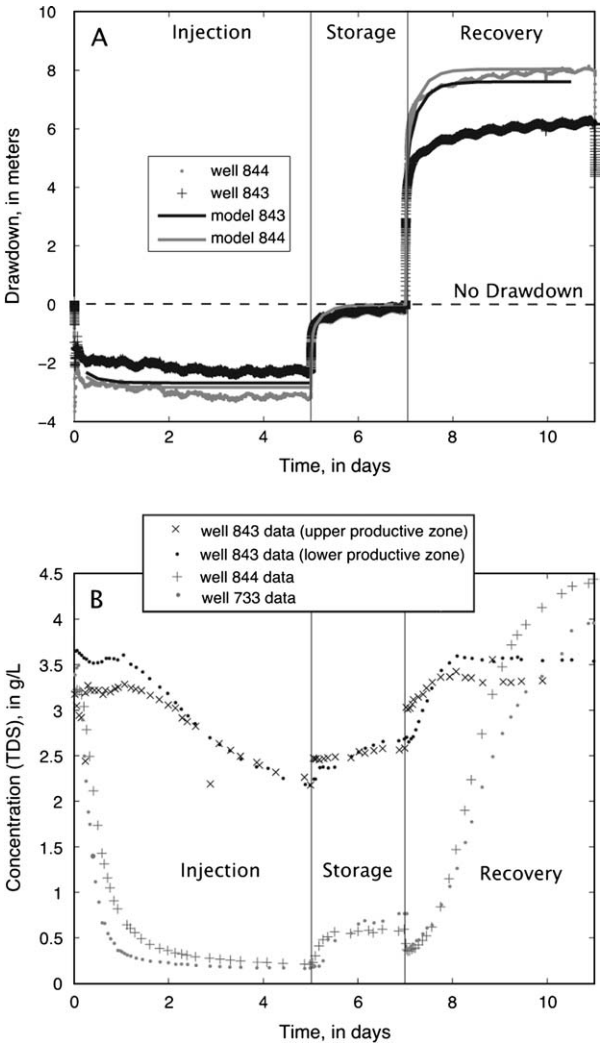

Figure 3. (A) Data from the 2005 test at the pilot study site and simulated results for drawdown over one ASR cycle. Local heterogeneity produces less connectivity between well 843 and the injection/pumping well. (B) Salinity (TDS) data from 2005 test over the ASR cycle. The injection concentration is 0.16 g/L. Lower connectivity between wells 736 and 843 is evident. Salinity rebounds during storage as solute is exchanged between fresh injected water and brackish water in immobile pore spaces. Salinity drops briefly again in wells 733 and 844 at the start of pumping (recovery), indicating that an immediate response to pumping as fresh water from adjacent mobile zones is advected through the observation wells. The salinity drop is not seen in well 843, presumably because well 843 is poorly connected to the pumping well relative to wells 733 and 844.

a brackish aquifer, we expect to see salinity drop during injection when the fresh water plume breaks through the zone being sampled. Conversely, salt concentration will rise during pumping as mixed water and brackish water are drawn back into the observation well; concentrations will reach the initial native water concentration if pumping continues long enough. Little change in concentration should occur during storage under advection-dispersion conditions as long as the observation well remains in the unmixed area of the injected fresh water bubble; however, salinity data from the 2005 ASR cycle deviate from the behavior expected given a conceptual model of advection-dispersion processes alone.

Salinity data from well 843 show a weaker response to the injection and recovery stresses applied on the system than do the other wells, consistent with the poor connection inferred from the head data. Salinity data from wells 733 and 844 share a nearly identical profile over the entire ASR cycle. An abrupt down-dip in salinity was observed in wells 733 and 844 on day 7 of the cycle in response to recovery pumping.

Evidence for RLMT at the Charleston Site

The salinity data show compelling evidence that RLMT processes may be affecting solute transport in the BM/SL Aquifer. This is most clearly evident in the rebound in salinity at wells 733 and 844 during the 2-d storage period (days 6 and 7) (Figure 3B). This rebound is recorded in salinity data from the observation wells. Colocated bulk electrical conductivity data, described in Singha et al. (2007), show comparatively little change. Bulk electrical conductivity measures both mobile and immobile fluids in the aquifer. The discrepancy in storage period behavior between mobile and bulk measurements suggests that local-scale solute exchange between the two porosity domains is responsible for the anomalous salinity rebound rather than advective upwelling of fluids from the confining units, as is proposed in earlier work (Petkewich et al. 2004).

We propose the following conceptual model to explain the field data (Figure 4): (1) during the injection period, relatively fresh water displaces brackish native aquifer water in the mobile pore spaces; (2) during storage, local, diffusive solute exchange occurs between the mobile and the immobile porosity domains, in the absence of substantial advection; and (3) during the pumping (recovery) period, water that has been degraded by diffusive mixing is recovered from the mobile zones of the aquifer and is replaced in the mobile pore spaces by brackish native aquifer water from beyond the "bubble" of injected water. To test this conceptual model and investigate its implications, we present a series of numerical flow and transport models to match the 2005 ASR data. Flow models are calibrated to the drawdown data, and SDM and DDM models with RLMT are used to simulate solute transport at this ASR site.

Numerical Modeling

A series of numerical models are used to simulate flow and transport in the BM/SL Aquifer for an ASR cycle identical to the one conducted in August 2005. Both SDM and DDM transport models are evaluated and used for parameter estimation and sensitivity analysis. We use well log data (Figure 2) to define the geometry of a three-dimensional finite-difference grid representing the productive zones and confining units of the site. MODFLOW-2000 (Harbaugh et al. 2000) is used to simulate flow, and MT3DMS (Zheng and Wang 1999) with particle tracking is used for transport simulations in this study.

Model Construction

The finite-difference grid is composed of 154 rows, 144 columns, and 4 layers, for a total of 88,704 block-centered

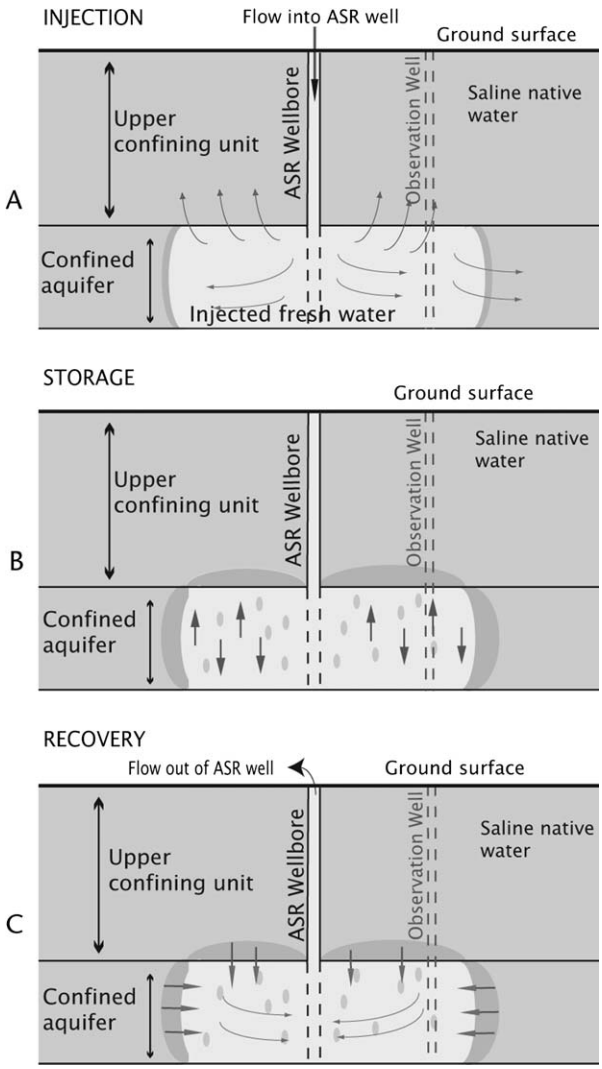

Figure 4. Conceptual model of RLMT processes over one ASR cycle. (A) Injected water flows through the mobile porosity zone of the aquifer into fractures in the confined aquifer and possibly fractures of the overlaying confining units. (B) During storage, brackish water in the immobile pore spaces mixes with injected fresh water in the confining unit. (C) When pumping commences, fresh water and mixed water are pulled through the aquifer.

nodes. The model is set up as a telescoping grid, with cells that are 0.5 m^2 around ASR well 736 and expand to approximately 17 m^2 at the boundaries. The model domain is 1 × 1 km. The boundaries of the grid are positioned at sufficient distance from our experiment site that they have minimal impact on the model solution over the timescales of interest. The small natural flow gradient of 5.0×10^{-4} m/m (Petkewich et al. 2004) is ignored, and the model domain has constant hydraulic head boundaries on all sides fixed at the top of the system. The fixed-head and salinity boundary conditions allow the system to return to equilibrium with respect to both water level and salinity during storage periods. Because each of the two productive zones in the BM/SL Aquifer carries a similar proportion of flow and is surrounded by confining units (Petkewich et al. 2004), we simplify the model domain by presenting it as one 6-m-thick layer of relatively high hydraulic conductivity (K) with 5-m-thick over- and underlying confining units. There is no assumed variation in layer thickness.

We simulate the study conditions, where fluid is injected at 174 m^3/d for 5 d, stored for 2 d, and recovered at 468 m^3/d for 4 d. Flow into each model layer is weighted by transmissivity, with the vast majority entering and exiting the system through the productive zone layer. The hydraulic conductivity is considered isotropic in the model. The initial estimates of hydraulic properties used in our models come from aquifer tests performed at the pilot study and phase II sites (Campbell et al. 1997; Petkewich et al. 2004). Based on field observations, we assume a salinity of 160 mg/L for injected water and a background salinity of 3300 mg/L for the aquifer. There is some spatial variability in the initial, preinjection salinities at wells 843, 844, and 733. The salinities range between 3100 and 3600 mg/L, so we generalize this to one initial salinity condition of 3300 mg/L for the entire system.

Buoyancy stratification effects, which may in some cases degrade efficiency by causing migration of the injected fresh water bubble, are not considered in this study. Previous work at ASR sites in Florida showed that substantial stratification is not expected when the targeted aquifer is thin and native ground water salinity is less than 5000 mg/L (Reese 2002). These findings have been applied to previous ASR tests in the BM/SL Aquifer (Petkewich et al. 2004). Additionally, we assume a nonsorbing system, where salinity acts as a conservative tracer similar to chloride. This assumption is justified by previous work that confirmed the conservative nature of fluid electrical conductivity (and, in turn, salinity) in the BM/SL Aquifer (Campbell et al. 1997).

Estimation of Parameters Controlling Flow

The flow model is calibrated to hydraulic head data from wells 843 and 844 to infer K and specific storage (S_s) with the aid of an analytical solution for a homogeneous system with an equivalent ASR cycle. Although drawdown data are not available at well 733, we consider the flow behavior to be similar to well 844 because the wells' salinity profiles are similar. Table 1 lists the best-fit parameters for the flow model. The low K of the confining units is based on estimates by Petkewich et al. (2004), and K in the aquifer is adjusted to calibrate the model. A uniform S_s is estimated for the entire model domain. The calibrated model successfully reproduces the water-level response at well 844 during injection, storage, and recovery (Figure 3A) but does not match the hydraulic head data for well 843 as well. No single transmissivity value results in good matches to hydraulic heads observed at both wells 844 and 843, suggesting heterogeneity within the aquifer over distances of several meters. Aquifer tests performed at this site between 1993 and 1995 suggest that anisotropy may also impact flow within the BM/SL Aquifer (Campbell et al. 1997). As mentioned previously, well 843 is poorly connected to well 736. Imposing a localized zone of very low K around well 843 was found to be moderately successful.

Table 1
Best-Fit Values for the SDM and DDM at an ASR Site in Charleston, South Carolina

	SDM Aquifer (no heterogeneity)	SDM Confining Units	DDM Aquifer Inner Zone	DDM Aquifer Outer Zone	DDM Aquifer Low-Connectivity Zone	DMM Confining Units
K (m/d)	1.0	0.05	100	1.0	0.075	0.05
S_s (/m)	5×10^{-6}	5×10^{-6}	5×10^{-6}	5×10^{-6}	5×10^{-6}	5×10^{-6}
θ_m	NA	NA	0.025	0.025	0.025	0.025
θ_{im}	NA	NA	0.25	0.25	0.25	0.25
β (/d)	NA	NA	0.012	1×10^{-4}	0.01	1×10^{-4}
Longitudinal dispersivity (m)	0.1	0.1	NA	NA	NA	NA
θ_e	0.03	0.03	NA	NA	NA	NA

Note: NA, not applicable. The SDM is a single-porosity domain model and the DDM is a dual-domain porosity model to simulate RLMT.

Estimation of Parameters Controlling Transport: Single-Domain Model

Salinity data from wells 733 and 844 were used to calibrate an SDM (advection-dispersion only) for longitudinal dispersivity and θ_e. Transverse dispersivities (α_T) were fixed at $\alpha_T = 0.10\alpha_L$ (longitudinal dispersivity) for all simulations. The best-fit values obtained for the SDM were an α_L of 0.1 m and a θ_e of 0.03 over the entire model domain. Figure 5A shows the resulting best fit for the SDM. The simulated salinity profile is similar for all three observation wells because of the lack of heterogeneity imposed on the aquifer zone. We are not able to reproduce the salinity rebound during storage days 6 and 7 with the SDM; this suggests that processes in addition to dispersive mixing at the front of the fresh water bubble are responsible for the transport behavior observed at observation wells 733 and 844. Geophysical data from Singha et al. (2007) suggest that advective upwelling of fluids is unlikely to be a controlling process because bulk electrical conductivity remains constant despite changes in observed salinity. The apparent bulk conductivities from conduction simulations fit colocated point values as described in Singha et al. (2007).

Estimation of Parameters Controlling Transport: Dual-Domain Model

The model described previously was used as the basis for exploration of RLMT processes in a DDM. The best-fit porosity value from the SDM is helpful, because it gives an idea of the amount of total advective porosity (θ_m) that might be expected in the DDM. Salinity data from wells 733 and 844 were used to calibrate a DDM with RLMT for mass transfer coefficient β and mobile and immobile porosity (θ_m and θ_{im}, respectively). The chemical reaction package of MT3DMS was used to simulate two porosity domains in the model (Zheng and Wang 1999). The same pumping scheme, boundaries, and initial conditions are used as in the SDM.

Application of the DDM is necessary to reproduce the salinity behavior observed during the storage period (Figure 5B). Table 1 shows the best-fit values for β, θ_m, and θ_{im}. Diffusive transport from the immobile porosity zone to the mobile zone reproduces the salinity rebound observed at the start of storage. The down-dip observed in wells 733 and 844 at the start of pumping must result from reintroduction of low-salinity fluids from over- or underlying confining units or dead-end or terminal fracture spaces within the BM/SL Aquifer itself. We interpret this down-dip as the result of injected fresh water reaching mobile pore space that is predominantly isolated from the immobile zones. This would occur primarily at the tip or terminus of fractures, where fluids are pushed into the confining units with lower mass transfer rate. This injected fluid remains relatively unmixed and is pulled back as low-salinity water past wells 844 and 733 at the start of pumping, resulting in the observed down-dip. Fracture termini likely occur throughout the aquifer layer, but only those in the vicinity of the sampling boreholes would contribute to the down-dip measured in those boreholes. Consequently, in an attempt to simulate termini associated with our salinity data, we place the edge of the inner zone near the simulated observation wells.

In our numerical model, the fracture networks connecting ASR well 736 to observation wells 733 and 844 are represented as a high K zone (the inner zone in Figure 6). An outer zone, with a lower K (Table 1), encloses the high K zone and extends to the model boundaries. The observation wells are positioned at cells adjacent to the border of the inner and outer zones to simulate the effect of fracture termini on the salinity measured at the boreholes. A low β value of 1×10^{-4}/d is applied to the entire model domain except for the inner zone, where higher mass transfer is expected. The best-fit values in Table 1 produce the storage period rebound observed in the data, and the lower β in the outer zone produces the down-dip at the start of recovery on day 7. The compartmentalization of the aquifer layer into inner and outer zones has a negligible impact on the model fit of drawdown at the observation wells, regardless of the 100-fold discrepancy in K between the two zones; the overall flow regime of the model is dominated by the much larger outlying zones that are in connection to the fixed-head boundaries.

We hypothesize that the lack of connectivity that was observed in drawdown and salinity data at well 843 is due to relatively few fracture pathways connecting this

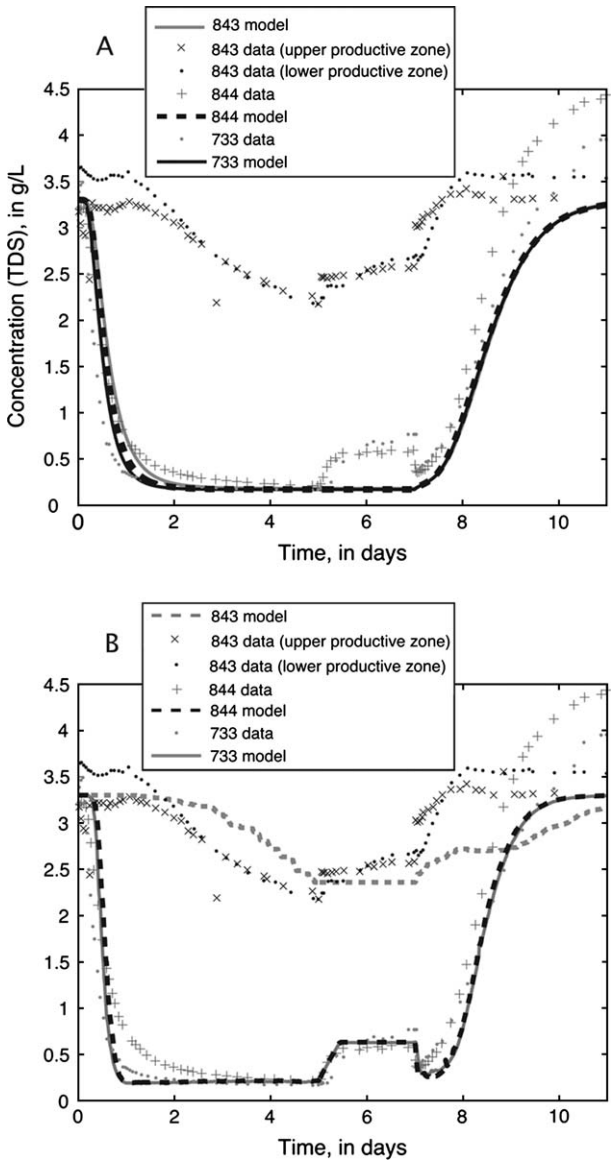

Figure 5. (A) Fit of SDM to salinity data from observation wells 843, 844, and 733. Note that storage period behavior is not reproduced in this model. Well 843 is not modeled as within a low-connectivity zone. (B) Fit of DDM to salinity data from the same three observation wells, with storage period salinity rebound and down-dip at wells 733 and 844. Well 843 has been isolated in a low-connectivity zone.

observation well with well 736. To test this, we imposed a zone of low K around well 843 in the DDM to reproduce the lack of connectivity between wells 736 and 843 (Figure 6). Our zonation of the localized low K zone around well 843 is arbitrary but results in a drawdown fit difference of less than 1 m between wells 843 and 844 with negligible effects on the modeled transport behavior at wells 733 and 844. Lowering K several orders of magnitude in the low-connectivity zone improves the fit to drawdown but not salinity at well 843. The DDM fits well 843 rather poorly. Achieving a perfect fit to all three wells would most likely require the imposition of anisotropy or statistical heterogeneity on the system and is beyond the scope of this study; instead, we focus primarily on the anomalous transport behavior observed in wells 844 and 733, which are in good hydraulic communication with ASR well 736. The effect of anomalous processes is also less apparent in well 843; therefore, we do not fully explore the sensitivity of well 843 to transport parameters.

The DDM is an improvement over the SDM in two important respects: (1) the DDM is able to reproduce the salinity rebound during storage, which is explained by diffusive solute exchange between two porosity domains; and (2) the DDM can reproduce the anomalous down-dip observed at the start of the pumping, which is explained by variability in the mass transfer rate coefficient between the fractures and the matrix. Our best-fit value of β in the inner zone is 1.2×10^{-2}/d. Assuming open water diffusion based on Cl^-, the primary anion in the pore fluid (Campbell et al. 1997), results in a β value corresponding to a diffusive length of 6 cm. To relate β to a diffusive length, we consider mass transfer to be similar to open water diffusion and apply the known diffusion coefficient (i.e., Cl^-) to approximate the length scale over which diffusion or mass transfer occur.

Sensitivity Analyses of DDM

We use the DDM model with a range of RLMT parameters to evaluate the sensitivity of the simulated salinity response over an ASR cycle. We perform sensitivity analyses for β, θ_m, and θ_{im}. The model results presented in Figures 5A and 5B are from the mobile porosity zone only because our salinity data are representative of only mobile fluids in the BM/SL Aquifer.

Root mean squared deviation (RMSD) is a dimensionless measure of the difference between values predicted by a model and actual observed values. In this study, these two sets of values are the mobile salinity data from well 844 and the model results for mobile concentration at the node representative of this well. A higher deviation, or larger value of RMSD, indicates less agreement between the model and the field data for a given location. RMSD values ranged from 0.5 for the best-fit parameters to as much as 1.5 for very inaccurate models.

Mass Transfer Coefficient, β

The sensitivity of the DDM to β is illustrated in Figure 7A. β is estimated only for the inner zone, where we observe the salinity rebound during storage. This zone represents the terminal fracture zones in contact with the wells as well as all interfaces between mobile and immobile fluids in the aquifer. Outer zone β values are kept constant at 1×10^{-4} /d to maintain low solute exchange in this zone; this is reasonable given the lower fracture density above and below the productive zones in the BM/SL Aquifer and is needed to generate the down-dip at day 7. Regardless, simulation results are relatively insensitive to β in the outer zone; the outer zone does not have a significant contribution to salinity results over a 2-d storage period. In the simulated injection period, salinity does not reach the injectant salinity of 160 mg/L when β is large ($>5 \times 10^{-2}$/d) because of fast exchange of solutes with the more saline immobile domain. The salinity rebound

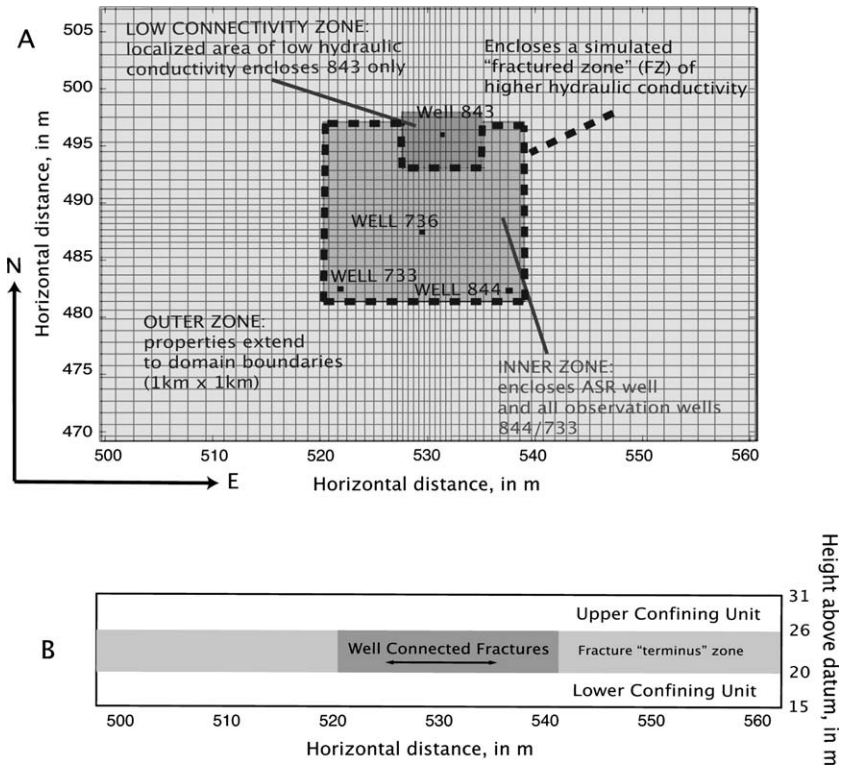

Figure 6. (A) DDM aquifer layer in map view. Observation wells are placed at the edge of a simulated "fracture zone" of high conductivity to reproduce the storage period salinity profile. An additional zone of heterogeneity is placed around well 843 to reproduce the lack of connectivity. (B) Cross section of the model domain showing the inner zone of fracture pathways connecting well 736 with wells 844 and 733 (dark gray), outer zone (light gray), and confining units (white).

also is sensitive to adjustment of β. Simulated storage period behavior is able to emulate the field data over only limited range of β (Figure 7A)—as described earlier, values of β that are too high or two low produce a system that acts as a single domain.

Porosities in this series of simulations are fixed to the best-fit values of $\theta_m = 0.025$ and $\theta_{im} = 0.25$ (Table 1). The relatively low θ_m/θ_{im} ratio provides a large reservoir of brackish native water that degrades single-cycle efficiency if diffusive transport of high-salinity pore fluids into the mobile fluids occurs quickly. Efficiencies are lowest when mobile water in the vicinity of the ASR well is degraded during storage, between β values of 1×10^{-2}/d and 0.5/d. However, efficiency can improve when there is flushing of high-salinity pore fluids out of the mobile zone adjacent to the ASR well during injection, at β values above 0.5/d.

Mobile Porosity, θ_m

We also test the sensitivity of the DDM to changes in θ_m. Well 844 is the reference point for all salinity data used in the sensitivity analysis. In this series of simulations, θ_m values for the entire model domain, not just the inner zone, are varied. β is fixed at 1×10^{-2}/d for the inner zone and 1×10^{-5}/d for the outer zone. θ_{im} over the entire model domain is fixed at 0.25, so θ_m and θ_t are subject to change.

As in the case of β, our DDM is able to match the mobile salinity data over only a relatively limited range of θ_m values. For θ_m above 0.05, we see very little rebound in salinity during the storage period; fluids in the mobile zone are more dilute because of a large θ_m/θ_{im} ratio. As the total volume of fluid in θ_m increases, so does the total mass of solute that can be removed from θ_{im} during injection. The result is a less saline immobile domain during the storage period that transports less solute into the mobile domain (Equation 2), so there is less observed rebound. The best-fit θ_m value was determined to be 0.025. This value is consistent with previous studies of fractured dolomite that used θ_m values between 0.01 and 0.05 in multiregion porosity models (Haggerty et al. 2001).

The lack of well-defined trend between single-cycle efficiency and changes in θ_m suggests that determining θ_m/θ_{im} may be more important for estimating efficiency at ASR sites where RLMT is affecting transport than θ_m or θ_e estimates alone. In brackish aquifers, recovered water quality will be degraded as long as immobile pore spaces make up significant portion of the θ_t.

Immobile Porosity, θ_{im}

Model sensitivity to θ_{im} is tested similarly to the evaluation of θ_m. Immobile porosities are adjusted for the entire model domain and β is fixed at 0.012/d (Table 1). The DDM used for this analysis does not appear to be sensitive to changes in θ_{im} during the injection and pumping phases. The salinity rebound during storage is greater as θ_{im} increases (Figure 7B). Below θ_{im} values of about 0.03, there is no observable rebound in the simulation, because there is little brackish water available in the

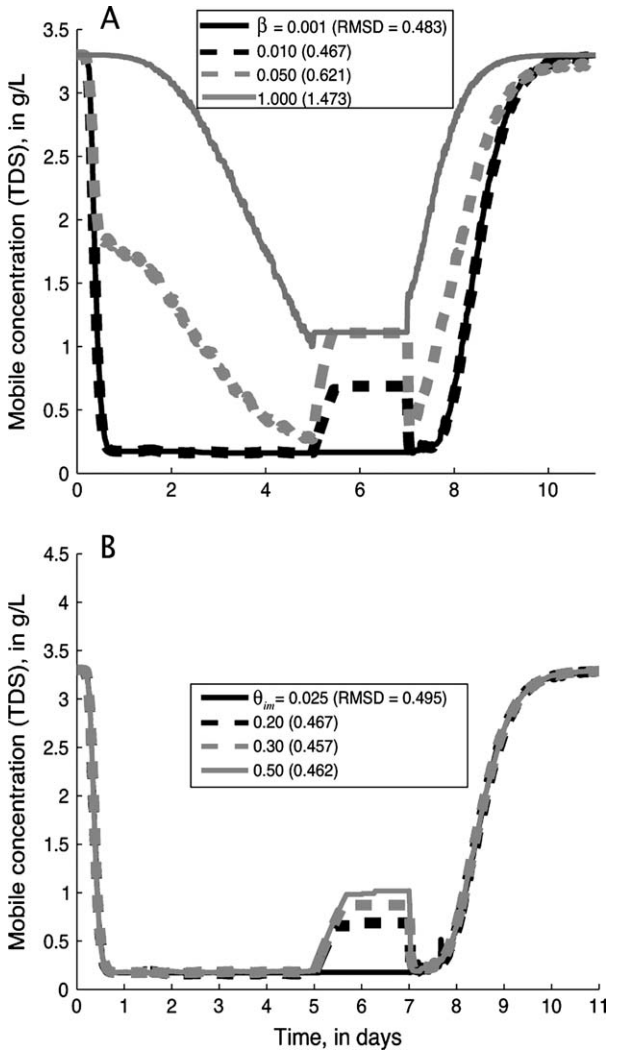

Figure 7. (A) Sensitivity of DDM to mass transfer coefficient, *β*. RMSD values are shown for each simulation (in parentheses), with higher RMSD indicating greater misfit to salinity data. Data and model results are for mobile pore fluid concentration at well 844. Higher *β* values correspond with faster solute exchange between porosity zones in the model. At the maximum and minimum *β* values, the DDM is similar to the SDM (results not shown), with a larger and smaller effective porosity θ_e, respectively. (B) Sensitivity of DDM to immobile porosity, θ_{im}. Salinity rebounding increases during the storage period as the total amount of immobile pore fluids increases.

immobile domain to diffuse out. We find that θ_{im} values of about 0.25 generate a model fit closest to the field data at well 844. This is consistent with a 2002 study at the phase II site (Figure 1) that estimated a θ_t between 0.10 and 0.30 (Petkewich et al. 2004). Our model calibration indicates that a θ_{im} of 0.25 and a θ_m of 0.025 provide the best fit to the data and are within the range of previously estimated values. Although θ_e in the SDM and θ_m in the DDM are not analogous parameters, the best-fit values obtained for both are similar, suggesting that the volume of pore space carrying advected fluid is similar under single- and dual-domain considerations. It may be appropriate to discuss sensitivity to θ_m/θ_{im} ratios with a fixed θ_t, and we do this in efficiency analyses for more simplified ASR models (see Conclusions section).

Effect of RLMT on ASR Efficiency

To simulate the effect of RLMT on ASR efficiency, we use the best-fit parameters from our DDM and SDM, excluding the heterogeneity that controls the down-dip described previously. Figure 8 shows modeled ASR efficiencies over 10 ASR cycles for both the SDM and the DDM. We use the same 5-2-4 d injection-storage-recovery cycle used in the field, iterated over 10 cycles. There is little change in efficiency over the entire 10 cycle time domain for the SDM because solute exchange occurs only along the mixing front of the fresh water plume; hence, the overall mass of solute in the system does not change substantially from cycle to cycle. In the DDM, the presence of enhanced quality water in the immobile domain after cycles 2 to 3 may contribute to the improved late-time efficiency; that is, the degradation of mobile fluids is offset by immobile fresh water in the vicinity of well 736. Early cycle efficiencies are between 40% and 50% for the best-fit DDM (Figure 8), which is higher than the maximum efficiencies reported by the pilot-scale four-cycle study from 2002, which generated efficiencies between 20% and 35% (Petkewich et al. 2004). This difference is most likely due to the long storage periods used in the earlier study, which were months rather than days, allowing more time for solute exchange, as well as effects of any regional ground water flow. The simulated salinity profile at well 736 over the 110-d run of the DDM shows decreasing rebound as solutes are progressively removed from the immobile domain, whereas the SDM results show a consistent salinity profile over all 10 cycles. Additionally, we observe a drastic increase in efficiency over the first three cycles of the DDM at higher β values due to very high exchange of solute degrading recovered water quality in early cycles (Figure 8). DDM efficiencies plateau at about 55%. The effects of dispersion in the SDM may be another reason for higher observed efficiencies in the DDM.

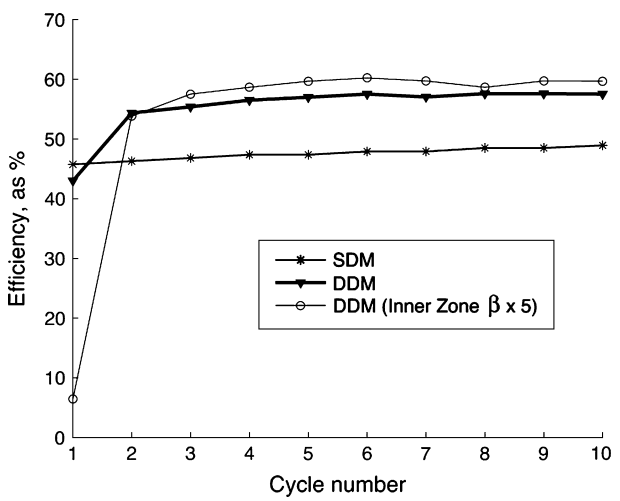

Figure 8. Efficiency over 10 ASR cycles for DDM and advection-dispersion model (SDM). All parameters are set to best-fit values listed in Table 1 unless otherwise noted. The DDM reaches a maximum efficiency after about three cycles, exceeding SDM efficiency.

Generalization of Results to Other Field Settings

To study the more general implications of RLMT for ASR, we simulate a simple, isotropic, homogeneous confined aquifer. The homogeneous K and S_s are based on analysis of the Charleston drawdown data. We also use the same initial conditions, boundary conditions, and injection, storage, and pumping scheme as in the heterogeneous model. This simplified model is used to evaluate the evolution of efficiency in a system with similar pumping conditions and storage timescales, using the same 500 mg/L salinity standard to estimate efficiency.

Figure 9A shows efficiency over 10 ASR cycles for a range of θ_m values. All other parameters are fixed to the values in Table 1, except β, which is 0.5/d. Although θ_{im} is fixed, θ_t is subject to change by altering θ_m. For most values of θ_m, the maximum efficiency is achieved after the first cycle. We see that maximum efficiencies over the θ_m range simulated approach 60%, similar to the SDM efficiencies in Figure 8. However, multicycle efficiencies are degraded as θ_m/θ_{im} decreases, reaching a minimum of approximately 40%, because of the greater potential for long-term degradation of injected water associated with a larger relative reservoir of brackish immobile pore fluids.

We also use the simplified model to evaluate recovery efficiency over a range of β values. θ_t is fixed at 0.10 with a θ_m/θ_{im} ratio of 1. In Figure 9B, there is small cycle-to-cycle fluctuation in efficiency, but an equilibrium efficiency is reached around cycle 8. By later cycles, the amount of solute transported out of the immobile domain during injection and storage and transported into the mobile domain during pumping does not change. In contrast to the porosity analysis, however, we see that maximum efficiencies of 50% are reached toward the upper and lower limits of β, with the lowest efficiencies of 25% to 30% occurring at β values between 0.1 and 0.01/d, corresponding to diffusive lengths between 2 and 6 cm. At lower β values, solute exchange is slow enough that recovered water is not substantially degraded by mixing with the more saline immobile fluids. With larger β values, fresh water pumped into the mobile pore spaces during injection is rapidly mixed with the immobile domain. This leaves low-salinity fluid in both the mobile and the immobile domains during storage, so that usable water is withdrawn during the early times of the recovery period, thus enhancing efficiency even during early cycles.

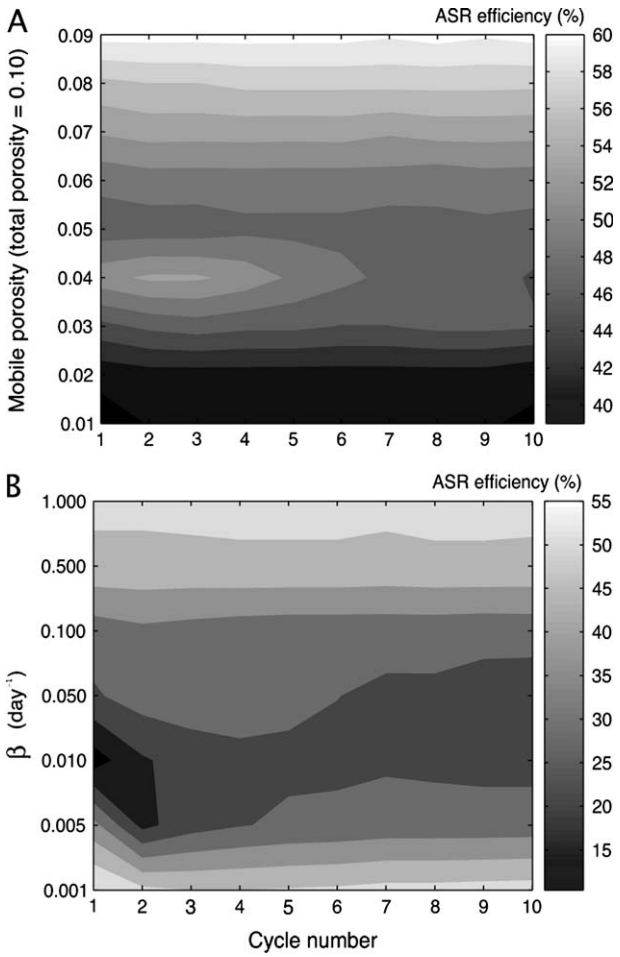

Figure 9. (A) Efficiencies over 10 ASR cycles for a range of mobile porosities in the simplified, homogeneous DDM. (B) Efficiencies over 10 cycles for a range of mass transfer coefficients (β) in the simplified, homogeneous DDM. Efficiency is highest at the maximum and minimum β, indicating a discrete range of conditions over which RLMT processes degrade efficiencies.

Discussion

In the absence of RLMT, the SDM is not able to reproduce observed transport behavior. In an SDM, there are a limited number of processes by which brackish native water would be encountered at observation wells during storage. One is dispersive mixing along the front of the injected fresh water bubble. We can rule this process out, because all three observation wells are located within the unmixed bubble of injected water, based on our observations. Advective flow into the wellbores from other areas of the aquifer or confining units could cause rebound; however, this explanation is contradicted by geoelectrical data, which do not indicate changes in bulk electrical conductivity (Singha et al. 2007). The success of the DDM in reproducing the storage period salinity rebound, the down-dip at the start of recovery, and the consistency with geophysical data (Singha et al. 2007) all strongly support our hypothesis that RLMT processes are affecting solute transport in the BM/SL Aquifer.

Diffusive transport from an immobile porosity zone in a DDM can explain the salinity rebound by RLMT. Our DDM was sensitive to both θ_m and β, and the storage period salinity behavior of our model is sensitive to adjustments of θ_{im}. Our sensitivity analyses show that there is a minimum θ_{im} value of 0.10, below which there is no salinity rebound during storage in the DDM. This suggests that it may be more important to determine the θ_t and θ_{im}/θ_m ratio than simply the total advective porosity at an ASR site. For this simulation, θ_{im} values between 0.20 and 0.50 provided a reservoir of brackish native water large enough to produce salinity rebound during storage that match the field data. This rebound, however, tends to cease beyond the first few ASR cycles in simulation, even at very high θ_{im} values, indicating that the reservoir of solute is flushed out with each subsequent cycle.

The equivalent porous media approach, in conjunction with a two-region porosity domain, appears to be an acceptable technique for modeling the fracture network connecting wells 733 and 844 with well 736. In our conceptualization of the fracture network, the wells lie near the edge a fracture zone, which results in the down-dip in salinity at day 8 at wells 733 and 844. This conceptualization is consistent with diffusive solute transport occurring at the contact area between the termini of mobile fracture networks and the stagnant pore spaces in the vicinity of the wellbore. During storage, a certain percentage of the mobile pore fluids remains relatively unmixed, and the outer zone in the model domain acts as a source for these unmixed fluids once pumping begins. In reality, any pore space within the aquifer or confining units containing water mobilized by well 736 may be a source of this relatively unmixed fluids; that is, the fresh water could return laterally from outside the fracture zone (as in our conceptualization), or vertically from over- and underlying confining units, or internally from dead-end fractures or poorly connected pore space.

The multicycle simulation results shown in Figure 8 suggest that, in general, RLMT degrades ASR efficiency during early cycles but may enhance it in later cycles. Indeed, simulated efficiencies for the DDM can exceed those of the SDM. It seems unlikely that the Charleston ASR site can achieve efficiencies as high as 60% over a single ASR cycle within the storage time used in this study, since our best-fit DDM produces low efficiencies for the first one to two cycles (Figure 8). Some of the native aquifer water in the BM/SL Aquifer is displaced by injection, and the quality of immobile water is improved by diffusive exchange during injection and storage. Although the θ_m values of the SDM and DDM presented in Figure 8 are the same, the θ_t of each system is different, yielding different total volumes of brackish aquifer water. It is reasonable to conclude, then, that the short-term degradation of efficiencies in the DDM may be because the DDM has a larger θ_t and a larger reservoir of brackish water in the system relative to the SDM.

Unlike the SDM, our DDM shows rapid improvement in efficiency over two to three cycles, until the net exchange of solute between the mobile and the immobile zones reaches an equilibrium condition. Therefore, in evaluating sites for ASR, it may be necessary to conduct several cycles of injection, storage, and recovery to obtain meaningful information to predict long-term ASR efficiency. Differing rates of solute exchange will degrade injected water quality on differing timescales; hence, the number of cycles necessary for evaluation will vary with site conditions and the values of parameters controlling mass transfer.

The best-fit β most likely represents the exchange of solute between the largest fracture pathways in the BM/SL Aquifer; however, a distribution of exchange rates may exist in an aquifer. The salinity data presented in Figure 3B show some evidence for this during the storage period rebound at wells 844 and 733. Whereas salinity at well 844 increases rapidly and levels off after day 5, the salinity at well 733 climbs more or less linearly between days 5 and 7. Although the profiles are similar, it is an important demonstration of the variability of solute exchange even within the small area that encloses the three observation wells. It is not known if other, slower diffusive pore scales are active in the BM/SL Aquifer, but these may serve to degrade efficiencies on timescales exceeding the 11-d ASR cycle evaluated here. Also, previous work indicates that issues such as cation exchange and regional ground water flow may affect efficiency in longer-term operations (Campbell et al. 1997; Petkewich et al. 2004), but such considerations are beyond the scope of this study. Nonetheless, for an emergency storage situation, in which the ASR system will be needed over the span of a few days, the large fracture β will dominate.

In addition to β, the ratio θ_m/θ_{im} also affects ASR efficiency (Figure 9A). How well an aquifer system approximates and underground storage tank depends on the communication between the aquifer's total porosity and the ASR well. When solute exchange is very high or very low, efficiencies on the order of 60% are achieved in our simulations; however, we see that for the scale of the system and cycle length imposed on it, there is a discrete range of diffusive length scales over which an ASR system like this will be less viable.

It should be noted that there are additional processes, not considered here, that might play roles in transport during the field experiments. For example, late-time salinity data climb above the modeled concentrations (Figure 5B). This increase in salinity may be due to introduction of mobile fluids from other areas of the aquifer under pumping or dissolution of the limestone bedrock (Plummer 1975). We extracted about 2.7 times the volume of water injected; hence, we may have drawn more saline fluids laterally or vertically toward the wells. Because the simulated aquifer is initially saturated with fluid containing 3300 mg/L TDS, no salinities higher than this occur anywhere in the model domain. Although we assumed uniform initial salinity for the modeling, in reality the background salinity may (1) be stratified by density or (2) vary spatially because of prior ASR experiments at the site or regional flow and transport.

Conclusions

ASR is emerging as a useful strategy for creating sustainable water resource infrastructure as well as for coastal aquifer management. ASR efficiency has previously been studied in the context of geochemical reactions, rock dissolution, and the redistribution of solute by advection. Past research has focused on dispersive mixing and permeability heterogeneity as the principal controls on efficiency. Here, we have demonstrated through numerical modeling and analysis of field experimental data that RLMT may (1) limit ASR single-cycle efficiency or possibly enhance multicycle efficiency; (2) explain observed changes in efficiency over multiple ASR cycles; (3) have important implications for practical evaluation of potential ASR sites; and (4) explain anomalous salinity rebound observed during storage cycles.

Sensitivity analysis indicates a discrete range of diffusive pore scales over which ASR efficiency is degraded by mass transfer; this range depends on the scale of the

system, imposed cycle length, and number of successive cycles. In the presence of RLMT, ASR efficiency will evolve over repeated cycles of injection, storage, and recovery, improving to a degree dependent on the controlling parameters, such as the rate coefficient and immobile porosity. With repeated injections of potable water, the native pore fluids in immobile zones will be replaced with higher quality water. For the Charleston site, numerical modeling results indicate that ASR efficiency will plateau at about 60% after three cycles. Initial site assessments may, thus, underpredict potential efficiency, and reliable site evaluation requires performance of multiple ASR cycles.

Acknowledgments

The authors are grateful for colleague reviews by Carole Johnson and Bruce Campbell (USGS), the comments of the *Ground Water* reviewers, and field support from Carole Johnson, Matthew Petkewich, and Kevin Conlon (USGS). This work was supported by the USGS Ground-Water Resources Program and American Chemical Society PRF 45206-G8.

References

Aucott, W.A., and G.K. Speiran. 1985. Potentiometric surfaces of the Coastal Plain aquifers of South Carolina prior to development. USGS Water-Resources Investigations Report 84-4208. Reston, Virginia: USGS.

Barker, J.A., T.E.J. Wright, and B.A. Fretwell. 2000. Pulsed-velocity method of double-porosity solute transport modeling. In IAHS Publication no. 262, 297–302.

Brothers, K., and T. Katzer. 1990. Water banking through artificial recharge, Las Vegas, Clark County, Nevada. *Journal of Hydrology* 115, no. 1–4: 77–103.

Campbell, B.G., K.J. Conlon, J.E. Mirecki, and M.D. Petkewich. 1997. Evaluation of aquifer storage recovery in the Santee Limestone/Black Mingo Aquifer near Charleston, South Carolina, 1993-95. USGS Water-Resources Investigations Report 96-4283. Reston, Virginia: USGS.

Coats, K.H., and B.D. Smith. 1964. Dead end pore volume and dispersion in porous media. *Society of Petroleum Engineers Journal* 4, no. 1: 73–84.

Eastwood, J., and P. Stanfield. 2001. Key success factors in an ASR scheme. *Quarterly Journal of Engineering Geology and Hydrogeology* 35, no. 4: 399–409.

Feehley, C.E., C. Zheng, and F.J. Molz. 2000. A dual-domain mass transfer approach for modeling solute transport in heterogeneous aquifers: Application to the macrodispersion experiment (MADE) site. *Water Resources Research* 26, no. 9: 2501–2516.

Flach, G.P., S.A. Crisman, and F.J. Molz. 2004. Comparison of single-domain and dual-domain subsurface transport models. *Ground Water* 42, no. 6: 815–828.

Fleming, S.W., and R. Haggerty. 2001. Modeling solute diffusion in the presence of pore-scale heterogeneity: Method development and an application to the Culebra dolomite member of the rustler formation, New Mexico, USA. *Journal of Contaminant Hydrology* 48, no. 3–4: 253–276.

Gaus, I., P. Shand, I.N. Gale, A.T. Williams, and J.C. Eastwood. 2002. Geochemical modeling of fluoride concentration changes during aquifer storage and recovery (ASR) in he Chalk aquifer in Wessex, England. *Quarterly Journal of Engineering Geology and Hydrogeology* 35, no. 2: 203–208.

Gleick, P.H. 2000. *The World's Water 1998-1999: The Biennial Report on Freshwater Resources*. Washington, D.C.: Island Press.

Griffioen, J.W., D.A. Barry, and J.Y. Parlange. 1998. Interpretation of two-region model parameters. *Water Resources Research* 34, no. 3: 373–384.

Haggerty, R., and S.M. Gorelick. 1998. Modeling mass transfer processes in soil columns with pore-scale heterogeneity. *Soil Science Society of America Journal* 62, no. 1: 62–74.

Haggerty, R., and S.M. Gorelick. 1995. Multiple-rate mass transfer for modeling diffusion and surface reactions in media with pore-scale heterogeneity. *Water Resources Research* 35, no. 10: 2382–2400.

Haggerty, R., S.W. Fleming, L.C. Meigs, and S.A. McKenna. 2001. Tracer tests in a fractured dolomite: 3. Double-porosity, multiple-rate mass transfer processes in convergent flow tracer tests. *Water Resources Research* 37, no. 5: 1143–1151.

Harbaugh, A.W., E.R. Banta, M.C. Hill, and M.G. McDonald. 2000. MODFLOW-2000, the U.S. Geological Survey modular ground-water model—User guide to modularization concepts and the ground-water flow process. USGS Open-File Report 00-92. Reston, Virginia: USGS.

Harvey, C.F., R. Haggerty, and S.M. Gorelick. 1994. Aquifer remediation: A method for estimating mass transfer rate coefficients and an evaluation of pulsed pumping. *Water Resources Research* 30, no. 7: 1979–1992.

Haselow, J.S., and R.A. Greenkorn. 1991. An experimental investigation of the effect of idealized heterogeneity on the dispersion of miscible fluids. *Water Resources Research* 27, no. 9: 2473–2482.

Haws, N.W., B.S. Das, P. Suresh, and C. Rao. 2004. Dual-domain solute transfer and transport processes: Evaluation in batch and transport experiments. *Journal of Contaminant Hydrology* 75, no. 3–4: 257–280.

Herczeg, A., K. Rattray, P. Killon, P. Pavelic, and K. Barry. 2004. Geochemical processes during five years of aquifer storage recovery. *Ground Water* 42, no. 3: 438–445.

Le Gal La Salle, C., J. Vanderzalm, J. Hutson, P. Dillon, P. Pavelic, and R. Martin. 2005. Isotope evolution and contribution to geochemical investigations in aquifer storage and recovery: A case study using reclaimed water at Bolivar, South Australia. *Hydrological Processes* 19, 3395–3411.

Lowry, C. 2004. Assessment of aquifer storage recovery; defining hydraulic controls on recovery efficiency at three representative sites in Wisconsin. M.S. thesis, Department of Geology and Geophysics, University of Wisconsin at Madison, Madison, Wisconsin.

Lowry, C.S., and M.P. Anderson. 2006. An assessment of aquifer storage recovery using ground water flow models. *Ground Water* 44, no. 5: 661–667.

Ma, L., and R.F. Spalding. 1996. Stable isotope characterization of the impacts of artificial ground water recharge. *Water Resources Bulletin* 26, no. 6: 1273–1282.

Mirecki, J.E., B.G. Campbell, K.J. Conlon, and M.D. Petkewich. 1998. Solute changes during aquifer storage recovery testing in a limestone/clastic aquifer. *Ground Water* 36, no. 3: 394–403.

Molz, F.J., C. Zheng, S.M. Gorelick, and C.F. Harvey. 2006. Comment on "Investigating the Macrodipersion Experiment (MADE) site in Columbus, Mississippi, using a three-dimensional inverse flow and transport model" by Heidi Christiansen Barlebo, Marcy C. Hill, and Dan Rosbjerg. *Water Resources Research* 42, no. 10: W06603.

Parkhurst, D.L., and M.D. Petkewich. 2001. Geochemical modeling of an aquifer storage recovery experiment, Charleston, South Carolina. USGS Open-File Report 02-89. Reston, Virginia: USGS.

Pedit, J.A., and C.T. Miller. 1994. Heterogeneous sorption processes in subsurface systems. 1. Model formulations and applications. *Environmental Science and Technology* 28, no. 12: 2094–2104.

Petkewich, M.D., D.L. Parkhurst, K.J. Conlon, B.G. Campbell, and J.E. Mirecki. 2004. Hydrologic and geochemical evaluation of aquifer storage recovery in the Santee Limestone/Black Mingo Aquifer, Charleston, South Carolina, 1998-2002. USGS Scientific Investigations Report 2004-5046. Reston, Virginia: USGS.

Plummer, L.N. 1975. Mixing of sea water with calcium carbonate ground water. *Geological Society of America Memoir* 142, 219–236.

Pyne, R.D.G. 1995. *Groundwater Recharge and Wells*. Boca Raton, Florida: Lewis Publishers.

Rao, P.S.C., D.E. Rolston, R.E. Jessup, and J.M. Davidson. 1980. Solute transport in aggregated porous media. *Soil Science Society of America Journal* 44, no. 6: 1139–1146.

Reese, R.S. 2002. Inventory and review of aquifer storage and recovery in Southern Florida. USGS Water-Resources Investigations Report 04-0236. Reston, Virginia: USGS.

Singha, K., F.D. Day-Lewis, and J.W. Lane. 2007. Geoelectrical evidence of biocontinuum transport in groundwater. *Geophysical Research Letters* 34, no. 12: L12401.

Vanderzalm, J.L., C. Le Gal La Salle, J.L. Hutson, and P.J. Dillon. 2002. Water quality changes during aquifer storage and recovery at Bolivar, South Australia. In *Management of Aquifer Recharge for Sustainability*, ed. P.J. Dillon, 265–268. Lisse, The Netherlands: Swets & Zeitlinger.

van Genuchten, M.T., and P.J. Wierenga. 1976. Mass transfer studies in sorbing porous media I. Analytical solutions. *Soil Science Society of America Journal* 40, no. 4: 473–479.

Zheng, C., and G. Bennet. 2002. *Applied Contaminant Transport Modeling*. New York: John Wiley and Sons.

Zheng, C., and P.P. Wang. 1999. MT3DMS, a modular three-dimensional transport model for simulation of advection, dispersion, and chemical reaction of contaminants in groundwater systems; documentation and user's guide. U.S. Army Engineer Research and Development Center Contract Report SERDP-99-1. Vicksburg, Mississippi: U.S. Army Engineer Research and Development Center.